Clinical Imaging 58 (2019) 84–89

Contents lists available at ScienceDirect

Clinical Imaging

journal homepage: www.elsevier.com/locate/clinimag

Breast Imaging

Preliminary study: Breast cancers can be well seen on 3T breast MRI with a half-dose of gadobutrol

Amy N. Melsaether[a,*], Eric Kim[a], Eralda Mema[a], James Babb[b], Sungheon Gene Kim[b,c]

[a] Department of Radiology, NYU School of Medicine, 160 E34th St, 3rd Floor, New York, NY 10016, United States of America
[b] NYU School of Medicine and Center for Advanced Imaging and Innovation, (CAI2R), NYU School of Medicine, 660 1st Ave, 2nd Floor, New York, NY 10016, United States of America
[c] Bernard and Irene Schwartz Center for Biomedical Imaging Department of Radiology, NYU School of Medicine, 660 1st Ave, 2nd Floor, New York, NY 10016, United States of America

ARTICLE INFO

Keywords:
Breast MRI
Low-dose
Half-dose
Gadolinium
Breast cancer
Gadobutrol

ABSTRACT

Background: Dynamic contrast enhanced (DCE) breast MRI is highly sensitive for breast cancer and requires gadolinium-based contrast agents (GBCA)s, which have potential safety concerns.
Purpose: Test whether breast cancers imaged by 3T DCE breast MRI with 0.05 mmol/kg of gadobutrol are detectable.
Methods: Analysis of 3T DCE breast MRIs with half dose of gadobutrol from patients included in an IRB-approved and HIPPA-compliant prospective study of breast PET/MRI. Between 11/7/2014 and 3/2/2018, 41 consecutive women with biopsy-proven breast cancer that was at least 2 cm, multi-focal or multi-centric, had axillary metastasis, or had skin involvement who gave informed consent were included. Two breast radiologists independently recorded lesion conspicuity on a 4-point scale (0 = not seen, 1 = questionably seen, 2 = adequately seen, 3 = certainly seen), and measured the lesion. Size was compared between radiologists and with size on available mammogram, ultrasound, MRI, and surgical pathology. Inter-reader agreement was assessed by kappa coefficient for conspicuity. Lesion size comparisons were assessed using the Spearman rank correlation.
Results: In 40 patients (ages 28.4–80.5, 51.9 years), there were 49 cancers. 10.1% of lesions were 1 cm or less and 26.5% of lesions were 2 cm or less. Each reader detected 49/49 cancers. Conspicuity scores ranged from 2 to 3, mean 2.9/3 for both readers ($p = 0.47$). Size on half-dose 3T DCE-MRI correlated with size on surgical pathology ($r = 0.6$, $p = 0.03$) while size on mammogram and ultrasound did not ($r = 0.25$, $p = 0.46$; $r = 0.25$, $p = 0.42$).
Conclusion: All breast cancers in this cohort, as small as 0.4 cm, were seen on 3T DCE breast MRI with 0.05 mmol/kg dose of gadobutrol.

1. Introduction

1.1. Breast cancer screening

Mammogram is the standard of care for breast cancer screening [1,2]. However, DCE breast MRI is highly sensitive and has been shown to double cancer detection over mammogram and ultrasound combined in elevated risk women [3,4] and has shown to achieve incremental cancer detection rates of up to 22.6 per 1000 MRIs in normal risk women, with cancer yields among all four breast densities [5]. MRI detects cancers of average smaller sizes and lower rates of nodal metastases than cancers detected on physical exam, mammography, or ultrasound [3–5]. These smaller, node-negative cancers are associated with less invasive treatments and better long-term disease-free survival rates [6,7]. DCE breast MRI screening is now indicated for breast cancer screening in women with a 20% or greater lifetime risk of breast cancer and in many women with a personal history of breast cancer [8–12].

1.2. Gadolinium

The need for gadolinium-based contrast agents (GBCA)s is one obstacle to widespread screening with DCE-MRI. Other obstacles including cost, availability, and imaging time are beginning be addressed by recent studies showing that short DCE-MRI protocols including a

* Corresponding author.
E-mail addresses: amy.melsaether@mountsinai.org (A.N. Melsaether), Eric.kim2@nyumc.org (E. Kim), Eralda.mema@nyumc.org (E. Mema), james.babb@nyumc.org (J. Babb), Gene.kim@nyumc.org (S.G. Kim).

https://doi.org/10.1016/j.clinimag.2019.06.014
Received 5 April 2019; Received in revised form 11 June 2019; Accepted 26 June 2019
0899-7071/ © 2019 Elsevier Inc. All rights reserved.

single pre- and post-contrast T1-weighted image set have sensitivities nearly equivalent to a full protocol breast MRI [13–15].

GBCAs render hypervascular tissues with increased vascular leakiness (i.e. cancers) brighter on T1-weighted images than surrounding less vascular tissues and are, at present, essential to breast MRI. In its free form, gadolinium is toxic as it interferes with calcium channels and protein binding sites [16,17]. Gadolinium ions are therefore chelated to a conjugate base into linear or macrocylic GBCAs, which allow for renal excretion. Recent studies have demonstrated gadolinium accumulation in the brain and bone [18,19] with repeated administrations, although no associated toxic effects have been shown. Accumulation appears to be greater with linear as compared with macrocyclic contrast agents [20,21], although with repeated administration, as is required for screening, macrocyclic agents have also demonstrated brain accumulation [19,22]. GBCAs may cause minor allergic and even rare anaphylactic reactions [23,24] and, in patients with renal failure (which may be uncommon in a breast cancer screening population), gadolinium administration may lead to nephrogenic systemic fibrosis [25]. Finally, increasing concentrations of excreted gadolinium have been documented in environmental water including tap water, with concentrations highest in areas with robust medical imaging [26,27].

In light of potential adverse effects, deposition within the body, and excretion into our environment, an as low as reasonably achievable (ALARA) approach to imaging with gadolinium makes sense. Recent studies have looked at reducing GBCA dose in MRI exams of the brain [28], prostate [29], and heart [30]. In the breast, there are two older studies looking at GBCA dose: one looked at multiple doses of linear GBCAs [31] of variable relaxivities and another compared a 0.1 mmol GBCA dose with a higher dose [32], but none have addressed a reduced dose of a macrocyclic agent such as gadobutrol.

The purpose of this study was to determine whether breast cancers are detectable on dynamic contrast enhanced (DCE) breast MRI at 3T with a reduced, 0.05 mmol/kg, dose of gadobutrol.

2. Materials and methods

2.1. Study

This study was approved by our institutional review board and was Health Insurance Portability and Accountability Act-compliant. Written informed consent was provided by all study participants prior to participation. Between 11/7/2014 and 3/2/2018 patients underwent a breast MRI at 3T with a half dose (0.05 mmol/kg) of intravenous (IV) gadobutrol (Gadavist, Bayer Healthcare Pharmaceuticals, Whippany, NJ) as part of a study of breast and whole-body PET/MRI in breast cancer patients. In this study, a half dose of gadobutrol was administered for the breast PET/MRI, and a second half-dose was administered later in the same day for the subsequently performed whole-body PET/MRI, which is not analyzed in this manuscript.

2.2. Inclusion criteria

To be referred for this study, patients had to have a core biopsy-proven, untreated breast cancer that: 1. measured at least 2 cm in maximum diameter, 2. was multi-focal or multi-centric on conventional imaging, 3. was associated with a biopsy proven ipsilateral axillary nodal metastasis, or 4. involved the skin. Exclusion criteria included failure to adhere to the exam protocol or a prior gadolinium injection within 24 h of this exam to ensure that no residual gadolinium would affect exam interpretation. [Gadobutrol has been shown to have a mean terminal half-life of 1.8 h (90% CI 1.33–2.13 h) and to show 98% renal excretion at 12 h after injection of 0.1 mmol/kg] [33].

To be included as a cancer, an index lesion needed to be verified by core biopsy. In cases of additional ipsilateral cancers, lesions with a positive fine needle aspiration biopsy or a decrease in size or disappearance on follow-up 3T DCE-MRI in response to neoadjuvant chemotherapy in parallel with the index lesion were included.

2.3. DCE-MRI

DCE-MRI was performed as part of a an 18F-fluorodeoxyglucose (FDG) positron emission tomography (PET)/MRI breast exam on a 3T mMR system (Biograph, Siemens Healthineers, Erlangen, Germany) with a dedicated multi-channel breast coil (Noras, Wurzburg, Germany), with the patient in prone position and the breasts in mild compression. Data from the PET portion of this exam was not included in this study. However, 555 MBq 18f-FDG was injected IV 45 min prior to these examinations.

DCE-MRI data were acquired by two separate T1-weighted imaging protocols during this study. The first 24 patients were imaged using a prototype radial stack-of-stars 3D spoiled gradient echo pulse sequence [34] with frequency-selective fat suppression, TR/TE = 3.27/1.39 ms, flip angle = 12°, resolution = 1.4 × 1.4 × 2.5 mm^3, image matrix size = 256 × 256 × 80. A total of 1497 spokes (6:29 min) were acquired to generate 5 frames of 3D images (78 s/frame using 299 spokes/frame) using the online image reconstruction provided by the manufacturer. After baseline acquisition of 78 s (299 spokes), a single dose of gadobutrol at 0.05 mM/kg body weight was injected at 2 mL/s, followed by saline flush with a power injector (Medrad, Indianola, PA), while the scan continued for another 5 min 11 s (1196 spokes). For the first 6 patients, sagittal images were sent to PACS. In accordance with an institutional change in scan orientation, axial images were sent to PACS for the next 17 patients.

As initial exams appeared successful, the decision was made to proceed with our clinical T1 sequence to provide more familiar images that could also be useful as comparison exams for our clinical radiologists. Thus, the 24th through 40st patients were imaged in the axial plane by using a three-dimensional volume-interpolated breath-hold examination (VIBE) sequence with repetition/echo times of 4.74/1.79 ms and flip angle of 10 degrees for four frames with fat suppression using spectral attenuated inversion recovery (SPAIR). The image matrix size was 448 × 448 × 192 with the resolution of 0.8 × 0.8 × 1.1 mm^3. After the first frame, a single dose of gadobutrol at 0.05 mM/kg body weight was injected at 2 mL/s, followed by saline flush with a power injector (Medrad, Indianola, PA). The total duration of the scan was 6:20 min, with 1:35 min for each frame. Images were sent to PACS.

2.4. Image interpretation

Two breast radiologists, A.M. with 10 years of experience and E.M. with one year of experience, independently reviewed each study, using the third or fourth frame of the radial MRI dataset and the first or second post-contrast VIBE dataset. Readers knew that each patient had a breast cancer but were not aware of the laterality, location with the breast, or whether there were additional cancers in the ipsilateral or contralateral breast. Readers were blinded to each other, the patient's pathology results, and prior imaging. Each radiologist recorded whether a lesion was detectable on a four-point scale (0 = not seen, 1 = questionably seen, 2 = adequately seen, 3 = certainly seen) and lesion size by measurement of the greatest extent of abnormal enhancement. Lesion size was recorded as a surrogate marker of confidence in that if both radiologists recorded similar measurements, it would follow that the abnormal enhancement had a clearly perceivable boundary. When a measurement discrepancy between readers changed the category of mass size, the measurement by Reader 1 was used, as reader one had many years more experience. Reader 1 also characterized each lesion as a mass, focus, or nonmass enhancement and graded background parenchymal enhancement (BPE) and fibroglandular tissue (FGT) on four-point scales as described in the BI-RADS lexicon [35]. In cases of combined mass and nonmass enhancement, the lesion was categorized as nonmass enhancement when the extent of nonmass enhancement was inclusive of the mass.

2.5. Data collection

The electronic medical record (Epic, Madison, WI) was reviewed for patient age, menopausal status, clinical history including breast cancer risk factors and whether the breast cancer presented clinically, tumor pathology including estrogen receptor (ER), progesterone receptor (PR), and human epidermal growth factor receptor (HER) 2 status, axillary nodal biopsy results, whether neoadjuvant therapy was given, and surgical type and pathology results including tumor size. Prior radiology studies including mammograms, ultrasounds, and MRIs were reviewed, after data collection, for image interpretation. Dates of these exams, whether breast cancers were seen, and sizes of the breast cancers that were seen were recorded.

2.6. Data analysis

Inter-reader agreement was assessed in terms of the size kappa coefficient for the ordinal assessment of conspicuity and using the intra-class correlation and concordance correlation for lesion size. Readers were compared in terms of lesion conspicuity and size using a Wilcoxon signed rank test. The comparisons were conducted using the sample as a whole and stratified by tumor characteristics.

The comparison of scan types in terms of BPE was based on a Mann-Whitney test without correction for age because according to a Mann-Whitney test there was no significant difference between scan types in terms of age.

The association of size from the half-dose study and size at surgical pathology with each other and with size on mammogram, ultrasound, and MRI was assessed using the Spearman rank correlation. Correlation between conspicuity and tumor size and grade was assessed by the Spearman rank correlation. The Fisher exact test was used to assess for difference in conspicuity rating as a function or morphology and receptor type.

3. Results

3.1. Patient characteristics

41 patients (ages 28.4 years to 80.5 years, mean 52.5 years), all female, met inclusion criteria including a cancer that measured at least 2 cm on conventional imaging (n = 37), breast cancer that was multifocal or multi-centric on conventional imaging (n = 8), breast cancer that was associated with a biopsy proven ipsilateral axillary nodal metastasis (n = 22), or breast cancer that involved the skin (n = 2). One patient (age 76.3 years) received a full dose of gadolinium and was excluded from the study. The final patient population included 40 patients, (ages 28.4–80.5 years, mean 51.9 years). All included patients had pathology records for the index lesion available. Patient characteristics including menopausal status, risk factors, amount of FGT and amount of BPE are listed in Table 1.

3.2. Cancer characteristics

There were 49 cancers in 40 breasts; 47 of these cancers were biopsy proven (43 by core biopsy, four by fine needle aspiration biopsy with real-time cytopathologist interpretation), and two responded in tandem with the index lesion following neoadjuvant chemotherapy (Fig. 1). Thirty-four patients had one cancer, four patients had two cancers each, one patient had three cancers, and one patient had four cancers, all in the ipsilateral breasts. Five cancers were 1 cm or less and 13 were 2 cm or less. Thirteen cancers presented as nonmass enhancement and 1 as a focus. Additional tumor characteristics are detailed in Table 2.

3.3. Lesion detection

All 49 cancers were seen by both readers, with an average conspicuity score of 2.9 ± 0.3 for reader 1 and 2.9 ± 0.3 for reader 2 (p = 0.47). The kappa for conspicuity was 0.61, consistent with substantial inter-reader agreement. Reader 1 rated 44 cancers certainly seen and 5 cancers adequately seen. Reader 2 rated 42 cancers certainly seen and 7 cancers adequately seen. Neither reader 1 nor reader 2 rated any cancers not seen or questionably seen.

None of the tumor characteristics assessed led to differences in conspicuity and lesion size measurements were nearly equivalent between readers (mean 3.3 cm, range 0.4–9.2 cm) for each reader (p = 0.43). The intra-class correlation was 1.0 and the concordance correlation was 1.0, consistent with substantial inter-reader agreement. (Table 3).

Table 1
Patient characteristics.

Patient characteristics		Number (%)
Age in years	28.4–80.4, mean 51.9	
Menopausal status	Pre-	19 (47.5)
	Post-	21 (52.5)
Risk	None	22 (55.0)
	BRCA 1	4 (10.0)
	Personal history breast cancer	2 (5.0)
	Prior atypia	1 (2.5)
	Family history breast cancer	14 (35.0)
	Family history ovarian cancer	1 (2.5)
Fibroglandular tissue	Almost entirely fat	5 (12.5)
	Scattered	11 (27.5)
	Heterogeneous	16 (40.0)
	Extreme	8 (20.0)
Background parenchymal enhancement	Minimal	23 (57.5)
	Mild	14 (35.0)
	Moderate	3 (7.5)
	Marked	0 (0)

3.4. Differences between radial imaging and VIBE

Average BPE was not significantly higher in the group imaged with VIBE as compared to the group imaged with the radial protocol (1.71 ± 0.77 vs. 1.35 ± 0.49, p = 0.138).

3.5. Available mammography, ultrasound, full dose DCE-MRI, and surgical pathology

Mammogram was available for 48 cancers and was performed between 0 days and 71 days (mean 25.0 days) prior to the study exam. One patient refused mammography. Ultrasound was available for all 49 cancers and was performed between 0 days and 71 days (mean 24.8 days) prior to the study exam. Full dose DCE-MRI was available for 12 cancers and was performed between 2 days and 32 days from the date of the study exam (mean 15.4 days). Surgical pathology was available for 13 cancers, with operation dates between 3 days and 30 days (mean 17.9 days) after the study exam. Surgical pathology was not available in 24 patients who underwent neoadjuvant chemotherapy between imaging and surgical treatment, 7 patients who transferred care, 3 patients who were not surgical candidates due to distant metastatic disease, and 1 patient who refused treatment.

3.6. Modality performance

Of the 49 cancers, half-dose MRI, mammogram, ultrasound, and full-dose MRI detected 100%, 68.8%, 98.0%, and 100%. No additional cancers were seen on surgical pathological evaluation. Lesion size on half-dose MRI (3.2 ± 2.0 cm) was similar on full-dose MRI (3.2 ± 2.6 cm) (p = 0.73), and at surgical pathology (2.1 ± 0.8 cm

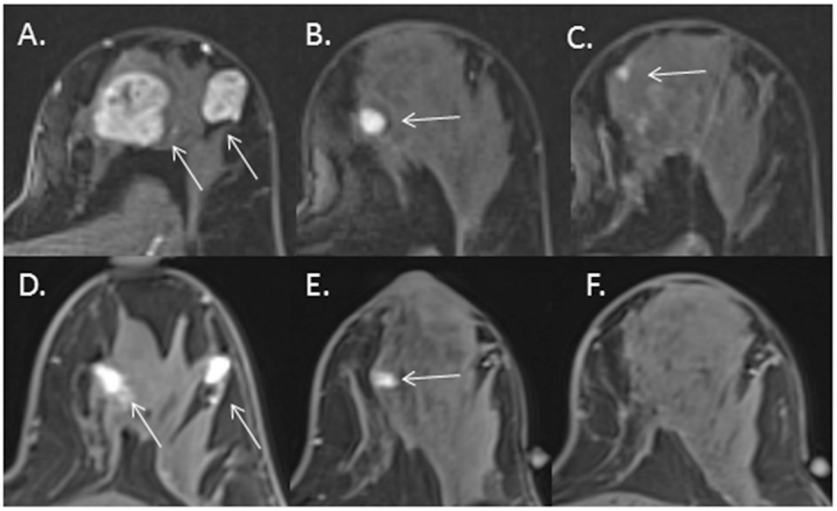

Fig. 1. A 43 year old BRCA1 + woman with a family history of breast cancer presented with a palpable mass in her left breast. She had a negative mammogram and ultrasound six months prior. She subsequently underwent core biopsy of the largest mass of three masses seen on initial ultrasound, which yielded high grade IDC. A second mass underwent find needle aspiration biopsy and yielded adenocarcinoma. Pre-chemotherapy half-dose DCE MRI demonstrates A. two heterogeneously enhancing masses (arrows) consistent with the biopsy proven cancers and b) an additional 1.1 cm mass (arrow) and c) and a 0.4 cm focus (arrow) that, on subsequent full-dose DCE-MRI, e) decreased (arrow) f) or disappeared d) in tandem with decrease in size in response to therapy of the biopsy-proven cancers (arrows).

Table 2
Tumor characteristics.

Tumor characteristics		Number (%)
Inclusion criteria	Core biopsy	43 (87.8)
	Fine needle aspiration biopsy	4 (8.2)
	Response to therapy	2 (4.1)
Palpable	Yes	36 (73.5)
	No	16 (32.7)
Size on MRI	0.4 cm–9.2 cm, mean 3.3 cm, median 2.8 cm	
	Up to 1 cm	5 (10.2)
	> 1 cm up to 2 cm	8 (16.3)
	> 2 cm up to 5 cm	27 (55.1)
	> 5 cm	9 (18.4)
Morphology	Mass	35 (71.4)
	Nonmass enhancement	13 (26.5)
	Focus	1 (2.0)
Type	DCIS	0 (0.0)
	IDC	42 (85.7)
	ILC	1 (2.0)
	Adenocarcinoma NOS[a]	4 (8.2)
	No information	2 (4.1)
Molecular grade	Low	1 (2.0)
	Intermediate	11 (22.4)
	High	31 (63.3)
	No information	6 (12.2)
Receptor status	ER/PR +	14 (28.6)
	ER + ; PR − or HER2 +	10 (20.4)
	ER/PR − and HER2 +	8 (16.3)
	ER/PR − and HER2 −	9 (18.4)
	No data	8 (16.3)
Axillary nodal metastasis	Yes	27 (67.5)
	No	13 (32.5)

[a] Results from fine needle aspiration biopsy.

Table 3
Lesion conspicuity and size per reader.

	Conspicuity Mean		Size in cm Range, mean	
	Reader 1	Reader 2	Reader 1	Reader 2
All cancers (n = 49)	2.9	2.9	0.4–9.2, 3.3	0.4–9.2, 3.3
Size				
Up to 1 cm (n = 5)	2.6	2.6	0.4–0.7, 0.6	0.4–0.8, 0.6
> 1 cm up to 2 cm (n = 8)	2.9	2.9	1.1–2.0, 1.7	1.2–2.2, 1.7
> 2 cm up to 5 cm (n = 27)	2.9	2.9	2.1–4.9, 3.1	1.8–5.0, 3.1
> 5 cm (n = 9)	3.0	2.8	5.1–9.2, 7.0	5.2–9.2, 7.0
Morphology				
Mass (n = 35)	2.9	2.9	0.6–6.3, 2.7	0.6–6.4, 2.7
NME[a] (n = 13)	2.9	2.8	0.7–9.2, 5.3	0.8–9.2, 5.3
Focus	Not enough data			
Molecular grade				
Low	Not enough data			
Intermediate (n = 11)	2.9	2.9	1.2–6.3, 3.3	1.4–6.4, 3.3
High (n = 31)	2.9	2.9	0.7–9.2, 3.9	0.8–9.2, 3.9
Receptor status				
ER/PR + (n = 14)	3.0	3.0	0.7–9.2, 3.6	0.7–9.1, 3.5
ER + ; PR − or HER2 + (n = 10)	2.8	2.8	1.8–8.1, 3.5	1.9–8.3, 3.5
ER/PR − and HER2 + (n = 8)	2.9	2.8	2.0–8.8, 4.1	2.0–9.2, 4.2
ER/PR − and HER2 − (n = 9)	3.0	2.9	1.4–8.4, 4.1	1.4–8.0, 4.1

[a] Nonmass enhancement.

vs. 1.9 ± 0.7 cm) (p = 0.56) for the subset of lesions imaged with full-dose MRI or that had surgical pathology available, respectively. In contrast, for lesions seen on mammogram or ultrasound, size on half-dose MRI was significantly different from size on mammography (3.4 ± 2.0 cm vs. 2.8 ± 1.8 cm) (p = 0.001) and size on ultrasound (3.3 ± 2.0 vs. 2.6 ± 1.4 cm) (p < 0.001) (Fig. 2). Further, size on half-dose MRI correlated with size on surgical pathology (r = 0.6, p = 0.03) whereas size on mammogram and ultrasound did not. Correlations for size on imaging with surgical pathology are presented in Table 4.

For lesions with surgical pathology available, mammogram yielded a smaller measurement than pathology in 8 cases (0.1 cm – 1.2 cm, 5% -43%) and a larger measurement than pathology in 3 cases. (0.1 cm – 2.4 cm, 14% - 200%). In 2 cases, the cancer was not seen. Ultrasound yielded a smaller measurement than pathology in 8 cases (0.1 cm – 1.5 cm, 5% - 46%), an equivalent measurement to pathology in 2 cases, and a larger measurement than pathology in 3 cases (0.1 cm – 0.6 cm, 8% - 50%). Half-dose MRI yielded a smaller measurement than pathology in 5 cases (0.1 cm – 0.4 cm, 5% - 14%), an equivalent measurement to pathology in 3 cases, and a larger measurement than pathology in 5 cases (0.1 cm – 0.6 cm, 4% - 50%).

4. Discussion

4.1. Half-dose MRI detects a range of cancers

This preliminary study is similar to early studies of DCE-MRI [36,37], and recent early studies of abbreviated protocol breast MRI [13,15] which also looked at the ability of MRI techniques to detect known breast cancers and is important as it lays groundwork for testing half-dose GBCA MRI in screening populations. Our detected cancers ranged from 0.4 cm to 9.2 cm and included 13 areas of nonmass enhancement and a single focus, suggesting that although this study

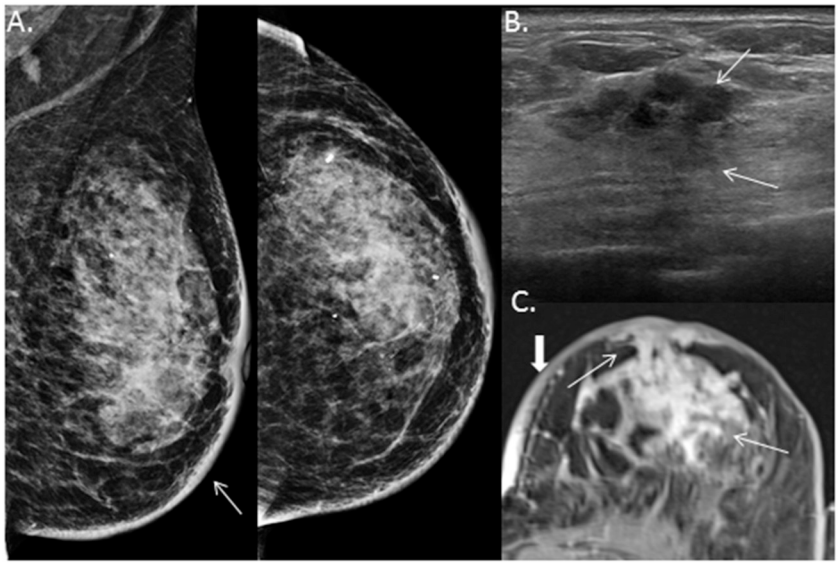

Fig. 2. A 74 year old woman with a remote history of right breast cancer presented with skin thickening and a palpable area of concern in her left breast. Skin involvement was demonstrated by punch biopsy. a) Mammogram shows skin thickening (arrow) best on the MLO view, without a discernable mass, b) ultrasound shows a 3.2 cm irregularly shaped mass with indistinct margins, and c) half-dose MRI demonstrates 8.2 cm of clumped and segmental nonmass enhancement (arrows) extending to and involving the nipple.

Table 4
Correlations between size at imaging and surgical pathology.

Measures correlated		r	p
Half-dose (n = 13)	Surgical pathology	0.60	0.03
Mammogram (n = 11, 2 occult)	Surgical pathology	0.25	0.46
Ultrasound (n = 13)	Surgical pathology	0.25	0.42
MRI (n = 5)	Surgical pathology	0.82	0.09

included predominantly larger cancers, the sensitivity of a reduced dose may not be limited by lesion size or morphology. Further, 2 readers measured lesions nearly identically, suggesting that clear borders were discernible with this reduced dose. It is possible that instead of preferring an exam generating the most conspicuity possible, radiologists could focus on finding an exam that uses the fewest resources to provide high detection.

4.2. Half-dose MRI appears to outperform mammogram and ultrasound

In the limited subset of patients with surgical pathologic correlation, there was significant correlation between size on the half-dose MRI and size at pathology, suggesting half-dose MRI accurately depicts tumor margins. Importantly, significant correlations were not seen between size on mammogram or ultrasound and size on pathology, suggesting that, like full-dose MRI, half-dose MRI outperforms both mammogram and ultrasound, even in this group of larger cancers. In Table 4, The full dose MRI appears to have a higher, although not significant, correlation with surgical pathology than the half-dose MRI. The authors believe this data point to be due to an outlier- a single cancer presenting as calcifications and nonmass enhancement which measured up to 3.6 cm on half-dose MRI and mammogram, but only 1.2 cm on final pathology. This cancer was not imaged with full dose MRI. Overall, these results are promising and suggest that a reduction in gadolinium dose may be possible without compromising cancer detection or evaluation of lesion extent.

4.3. Comparison with other low-dose studies

Our results compare favorably with a study by He et al. in which a low dose, 0.015 mmol/kg, of gadobentate demonstrated similar sensitivity (50%) and conspicuity score as a near complete dose (0.085 mmol/kg) for known prostate cancers [29]. Studies of the myocardium [30] and pituitary gland [38] have also suggested a half dose of gadolinium may be sufficient.

4.4. Limitations

There are several limitations to our study. The cancers in our study were larger, more advanced, of overall higher grade, and more likely to be triple negative or HER2 overexpressed than cancer in a screening population [5,7]. Further, no isolated DCIS and only one invasive lobular cancer was included.

Further, patients were referred to this study by their surgeon, who may have been biased in patient selection. Our study was performed with a relatively high relaxivity macrocylic GBCA and results may not be applicable to all GBCAs. Our study was performed as part of a breast PET/MRI on an integrated scanner, which is not usual for breast MRI. Our study was performed at 3T, however this field strength should not negatively affect applicability at 1.5T as gadolinium based contrast agent relaxivities are greater at 1.5T than at 3T [39]. Our study utilized a prototype radial scanning T1-weighted protocol for more than half of the patients that, in spite of no significant detection in lesion conspicuity, may have altered detection. Our study was not able to directly compare size on imaging with size on surgical pathology as most patients underwent neoadjuvant chemotherapy. Our study was also not able to directly compare half dose DCE-MRI with full dose DCE-MRI as most patients did not undergo full dose DCE-MRI.

5. Conclusion

This study demonstrates that breast cancers as small as 4 mm can be well seen with half-dose gadobultrol DCE-MRI. Further study is warranted to determine whether lower doses of GBCAs could be sufficient for DCE-MRI exams in broader patient groups.

Declaration of Competing Interest

No authors have any additional disclosures.

Acknowledgements

This work was supported in part by the National Institutes of Health (NIH) in the United States of America, grants R01CA160620, R01CA219964, P41EB017183.

References

[1] Hellquist BN, Duffy SW, Abdsaleh S, et al. Effectiveness of population-based service screening with mammography for women ages 40 to 49 years: evaluation of the Swedish Mammography Screening in Young Women [SCRY] cohort. Cancer 2011;117(4):714–22. Feb 15.

[2] Kopans DB. Beyond randomized controlled trials. Cancer 2002;94(2):580–1.

[3] Berg WA, Zhang Z, Lehrer D, et al. ACRIN 6666 Investigators. Detection of breast cancer with addition of annual screening ultrasound or a single screening MRI to mammography in women with elevated breast cancer risk. JAMA 2012;307(13):1394–404. Apr 4.

[4] Kuhl C, Weigel S, Schrading S, et al. Prospective multicenter cohort study to refine management recommendations for women at elevated familial risk of breast cancer: the EVA trial. J Clin Oncol 2010;28(9):1450–7. Mar 20.

[5] Kuhl CK, Strobel K, Bieling H, Leutner C, Schild HH, Schrading S. Supplemental breast MR imaging screening of women with average risk of breast cancer. Radiology. 2017;283(2):361–70. May.

[6] Noone AM, Howlader N, Krapcho M, et al [eds]. SEER cancer statistics review, 1975–2015, National Cancer Institute. Bethesda, MD, https://seer.cancer.gov/csr/1975_2015/, based on November 2017 SEER data submission, posted to the SEER web site, April 2018. Accessed 8/20/2018.

[7] Saadatmand S, Bretveld R, Siesling S, Tilanus-Linthorst MM. Influence of tumour stage at breast cancer detection on survival in modern times: population based study in 173,797 patients. Ned Tijdschr Geneeskd 2016;160:A9800.

[8] Saslow D, Boetes C, Burke W, et al. American Cancer Society Breast Cancer Advisory Group. American Cancer Society guidelines for breast screening with MRI as an adjunct to mammography. CA Cancer J Clin 2007;57(2):75–89. Mar-Apr.

[9] American College of Radiology. ACR practice parameter for the performance of contrast enhanced magnetic resonance imaging [MRI] of the breast. Reston, VA: American College of Radiology; 2018.

[10] Monticciolo DL, Newell MS, Moy L, Niell B, Monsees B, Sickles EA. Breast cancer screening in women at higher-than-average risk: recommendations from the ACR. J Am Coll Radiol 2018;15(3 Pt A):408–14. Mar.

[11] Tadros A, Arditi B, Weltz C, Port E, Margolies LR, Schmidt H. Utility of surveillance MRI in women with a personal history of breast cancer. Clin Imaging 2017;46:33–6. Nov-Dec.

[12] Brennan S, Liberman L, Dershaw DD, Morris E. Breast MRI screening of women with a personal history of breast cancer. AJR Am J Roentgenol 2010;195(2):510–6. Aug.

[13] Mango VL, Morris EA, David Dershaw D, et al. Abbreviated protocol for breast MRI: are multiple sequences needed for cancer detection? Eur J Radiol 2015;84(1):65–70. Jan.

[14] Kuhl CK, Schrading S, Strobel K, Schild HH, Hilgers RD, Bieling HB. Abbreviated breast magnetic resonance imaging [MRI]: first postcontrast subtracted images and maximum-intensity projection-a novel approach to breast cancer screening with MRI. J Clin Oncol 2014;32(22):2304–10. Aug 1.

[15] Heacock L, Melsaether AN, Heller SL, et al. Evaluation of a known breast cancer using an abbreviated breast MRI protocol: correlation of imaging characteristics and pathology with lesion detection and conspicuity. Eur J Radiol 2016;85(4):815–23. Apr.

[16] Lansman JB. Blockade of current through single calcium channels by trivalent lanthanide cations-effect of ionic radius on the rates of ion entry and exit. J Gen Physiol 1990;95:679–96.

[17] Biagi BA, Enyeart JJ. Gadolinium blocks low-threshold and high-threshold calcium currents in pituitary-cells. Am J Physiol 1990;259:C515–20.

[18] Olchowy C, Cebulski K, Łasecki M, et al. The presence of the gadolinium-based contrast agent depositions in the brain and symptoms of gadolinium neurotoxicity - a systematic review. Mohapatra S, ed. PLoS One 2017;12(2):e0171704.

[19] Murata N, Gonzalez-Cuyar LF, Murata K, et al. Macrocyclic and other non-group 1 gadolinium contrast agents deposit low levels of gadolinium in brain and bone tissue: preliminary results from 9 patients with normal renal function. Invest Radiol 2016;51(7):447–53. Jul.

[20] Lohrke J, Frisk AL, Frenzel T, et al. Histology and gadolinium distribution in the rodent brain after the administration of cumulative high doses of linear and macrocyclic gadolinium-based contrast agents. Invest Radiol 2017;52:324–33.

[21] Kanda T, Osawa M, Oba H, et al. High signal intensity in dentate nucleus on unenhanced T1-weighted MR images: association with linear versus macrocyclic gadolinium chelate administration. Radiology 2015;275(3):803–9. Jun.

[22] Bjørnerud A, Vatnehol SAS, Larsson C, Due-Tønnessen P, Hol PK, Groote IR. Signal enhancement of the dentate nucleus at unenhanced MR imaging after very high cumulative doses of the macrocyclic gadolinium-based contrast agent gadobutrol: an observational study. Radiology 2017;285(2):434–44. Nov.

[23] Prince MR, Zhang H, Zou Z, et al. Incidence of immediate gadolinium contrast media reactions. AJR Am J Roentgenol 2011;196(2):W138–43. Feb.

[24] Jung JW, Kang HR, Kim MH, et al. Immediate hypersensitivity reaction to gadolinium-based MR contrast media. Radiology 2012;264(2):414–22. Aug.

[25] Kaewlai R, Abujudeh H. Nephrogenic systemic fibrosis. AJR Am J Roentgenol 2012;199:W17–23.

[26] Bau M, Dulski P. Anthropogenic origin of positive gadolinium anomalies in river waters. Earth Planet Sci Lett 1996;143:245–55.

[27] Möller P, Paces T, Dulski P, Morteani G. Amthropogenic Gd in surface water, drainage system, and the water supply of the city of Prague, Czech Republic. Environ Sci Technol 2002;36:2387–94.

[28] Gong E, Pauly JM, Wintermark M, Zaharchuk G. Deep learning enables reduced gadolinium dose for contrast-enhanced brain MRI. J Magn Reson Imaging 2018;13. Feb.

[29] He D, Chatterjee A, Fan X, et al. Feasibility of dynamic contrast-enhanced magnetic resonance imaging using low-dose gadolinium: comparative performance with standard dose in prostate cancer diagnosis. Invest Radiol 2018;53(10):609–15.

[30] Galea N, Francone M, Zaccagna F, et al. Ultra low-dose of gadobenate dimeglumine for late gadolinium enhancement [LGE] imaging in acute myocardial infarction: a feasibility study. Eur J Radiol 2014;83(12):2151–8. Dec.

[31] Knopp MV, Bourne MW, Sardanelli F, et al. Gadobenate dimeglumine-enhanced MRI of the breast: analysis of dose response and comparison with gadopentetate dimeglumine. AJR Am J Roentgenol 2003;181(3):663–76. Sep.

[32] Heywang-Köbrunner SH, Haustein J, Pohl C, et al. Contrast-enhanced MR imaging of the breast: comparison of two different doses of gadopentetate dimeglumine. Radiology 1994;191(3):639–46. Jun.

[33] Staks T, Schuhmann-Giampieri G, Frenzel T, Weinmann HJ, Lange L, Platzek J. Pharmacokinetics, dose proportionality, and tolerability of gadobutrol after single intravenous injection in healthy volunteers. Invest Radiol 1994;29(7):709–15. Jul.

[34] Feng L, Grimm R, Block KT, et al. Golden-angle radial sparse parallel MRI: combination of compressed sensing, parallel imaging, and golden-angle radial sampling for fast and flexible dynamic volumetric MRI. Magn. Reson. Med. 2014;72(3):707–17.

[35] Morris EA, Comstock CE, Lee CH, et al. ACR BI-RADS® magnetic resonance imaging. ACR BI-RADS® Atlas, breast imaging reporting and data system. Reston, VA: American College of Radiology; 2013.

[36] Kuhl CK, Mielcareck P, Klaschik S, et al. Dynamic breast MR imaging: are signal intensity time course data useful for differential diagnosis of enhancing lesions? Radiology 1999;211(1):101–10. Apr.

[37] Kvistad KA, Rydland J, Vainio J, et al. Breast lesions: evaluation with dynamic contrast-enhanced T1-weighted MR imaging and with T2*-weighted first-pass perfusion MR imaging. Radiology 2000;216(2):545–53. Aug.

[38] Davis PC, Gokhale KA, Joseph GJ, et al. Pituitary adenoma: correlation of half-dose gadolinium-enhanced MR imaging with surgical findings in 26 patients. Radiology 1991;180(3):779–84. Sep.

[39] Shen Y, Goerner FL, Snyder C, et al. T1 relaxivities of gadolinium-based magnetic resonance contrast agents in human whole blood at 1.5, 3, and 7 T. Invest Radiol 2015;50(5):330–8. May.